A Review Paper on

Current Measurement and Noise Modeling in Solid State Nanopores

By

Dileep Dhakal

Submitted to

Prof. Dr. Matthias Winterhalter

December 2010

420511 Nanomolecular Science Graduate Seminar

Abstract

Selective and label free sensing of ions, bio-molecules and organic compounds are the major advantages of current monitoring along the solid state nanopore. This paper reviews the promising field of nanopore technology- noise modeling of current recording through solid state nanopores. Current across the nanopore is measured by resistive pulse sensing (RPS) technique. In RPS technique, a molecule is allowed to pass through the nanopore the molecule will then partially displace the conducting fluid inside the pore, resulting in the loss of ionic current across the nanopore.

Ionic current through the solid state nanopore is prone to wide varieties of noise. The paper will focus on the low frequency and high frequency noise modeling of the measured current by RPS technique and the method for reducing this noise. Label free detection is only possible by reducing the noise. Standard models are applied to understand low and high frequency noise in solid state nanopores. Additionally, PDMS coated nanopores are discussed being advantageous towards noise reduction.

Table of Contents

1. Introduction

Nanopores have attracted broad community of scientists, dedicated in the field of nanotechnology, biophysics and chemistry. Their common interest is concentrated on label free detection of molecules in the solution like, DNA sequencing [1], detection of proteins or polypeptides or nucleic acids or antibody-virus binding[2,3], nanoparticles [4], synthetic polymers [5], antibody-antigen [6,7] interaction and ions [8]. Label free detection is possible by pushing the desired molecule inside the nanopore and measuring the current across the nanopore. The incoming molecule displaces the conducting solution inside the nanopores which influences the detected current. The process of measuring current across the nanopore, due to displacement of conductive solution by the organic molecule is termed as resistive pulse sensing (RPS) technique. The detected current is highly influenced by the noise arising from nanopores, conductive solution and the measuring instruments.

Nanopores could be biological-origin like α-Haemolysin pore or formed by novel materials (carbon nanotubes or graphene nanopores) or fabricated on solid state nanopores (Si_3N_4 or SiO_2). Bio-nanopores had been centre of attraction, because of the ultrafast methodology for DNA sequencing. Biological nanopores were chemically engineered by techniques like mutagenesis [9], eventually many biosensors were developed [10]. Later, development of e-beam lithography, stable solid state nanopores were created on solid state substrate. Graphene nanopore have also huge potential in fabricating stable, uniform, thin and controlled nanopores [11], addition to SiO_2 or Si_3N_4 nanopores. Solid state nanopore exhibits every necessary feature required for a label free detection of organic molecules like, highly stable and controlled in diameters.

Solid State vs. Biological Nanopores

The major advantages of solid state nanopores compared with biological nanopores are the stability and control of diameters. Biological molecules are highly unstable in ambient condition and cannot withstand huge potential. Due to the advancement of lithography techniques nanopores with diameters in the order of 0.5nm has been successfully fabricated [12] [13]. Unfortunately, solid state nanopore exhibits huge low frequency flickering noise compared to biological nanopore. It is quite necessary to understand the noise behavior in solid state nanopore to design a label free detection of molecules. The following section deals with the major technological breakthrough towards fabrication of sub-nanometer solid state nanopores.

2. Fabrication of Solid State Nanopore

a. Focused Electron Beam Method

Focused electron beam method was first proposed by a team at Kavli Institute of Nanoscience, Delft University of Technology, where controlled nanopores (size upto 0.4nm) with gold electrodes were fabricated [13].

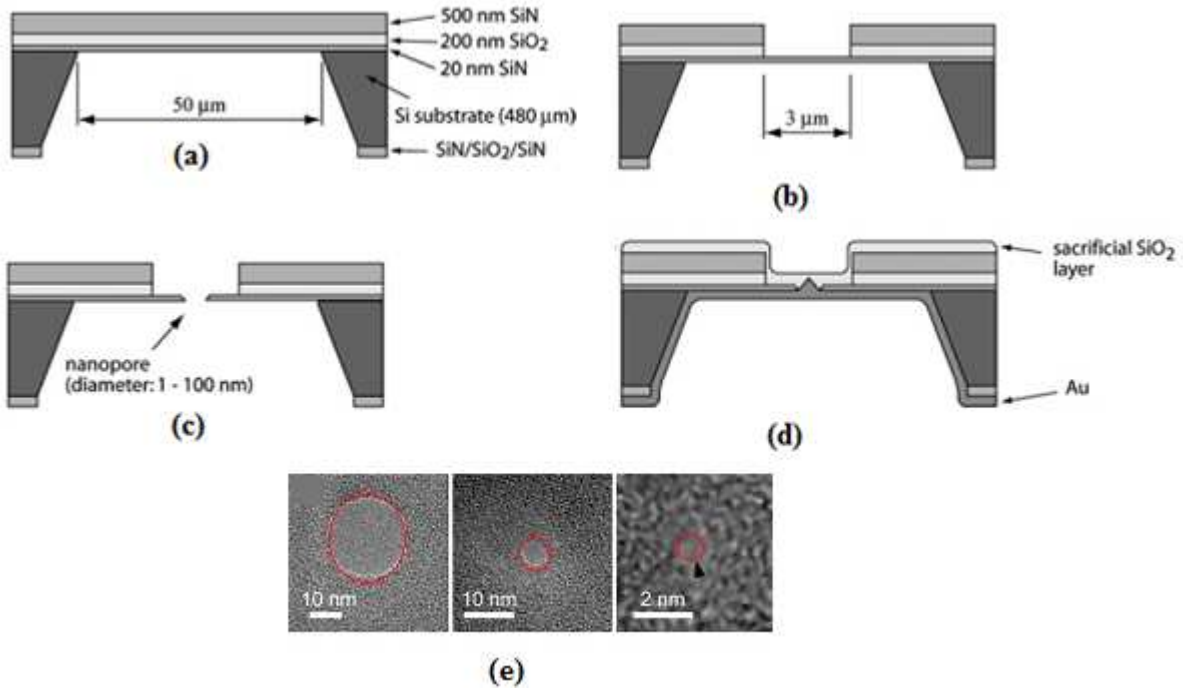

Figure 1: (a - d) Major steps involving in the fabrication of a nanopore in SiN layer by focused electron beam method. (e) Fabricated nanopores with diameter of 12, 2.5 and 0.4nm. [13]

In this method a focused electron beam is applied on the silicon nitride membrane with an intensity of 10^{-8}-10^{-9} e/nm^2. High intensity electron beam (100 to 300 KeV) breaks the covalent bond and causes Si and N atoms to be sputtered away into the vacuum. The major steps involves are: (a) Chemical vapor deposition (CVD) of SiN, SiO_2 and SiN layers on both surface of Silicon substrate. The back surface is carefully etched by KOH resulting in a large 50µm exposed SiN surface. (b) Etching away 3µm of SiN and SiO_2 layer from front surface of silicon substrate. (c) It is followed by applying a tight focused beam to SiN surface resulting approximately 0.4-100nm of SiN hole. (d) Final step involves is the deposition of SiO_2 layer by sputtering and evaporation of Au layer. When SiO_2 sacrificial layer is etched away by the buffered HF we get a pyramidal nanopore structure. The major advantage of this method is on spot observation of the nanopore during e-beam lithography process.

b. Ion Beam Sculpting

Ion beam sculpting method was first proposed by the team at Harvard University in 2001 [12]. The method applies a feedback-controlled sputtering system which provides the fine control over ion beam exposure and temperature of the sample.

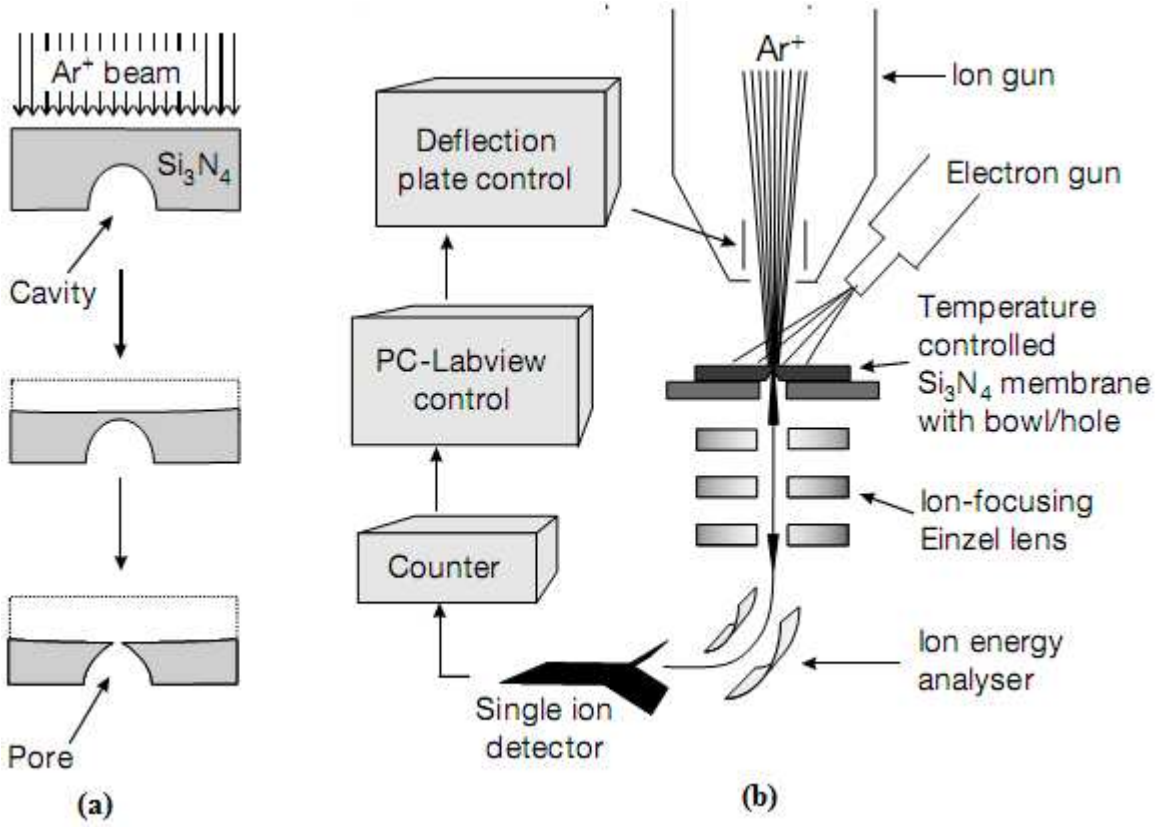

Figure 2: (a) Sputtering involves exposure of high energy argon beam to the Si_3N_4 sample. This high energy argon beam removes a thin layer of Si_3N_4 resulting a small nano pore. (b) Experimental setup involves sputtering unit and detector unit. Single ion detector sends the feedback signal for deflection of high energy argon source on the sample [12].

Figure 3: (a) Initial 61 nm pore on Si_3N_4 (b) 1.8nm pore formed after sputtering with argon ions. [12]

3. Current Measurement in Solid State Nanopore

RPS technique is the soul of current measurement across the solid state nanopore. In this technique, when molecule passes through a pore, it partially displaces the conducting fluid inside the pore (fig. 4). Hence, transient increase in the pore's electrical resistance is observed. Finally, the detected current would sharply decrease (fig. 5(c)). R. W Deblois and C. P. Bean calculated the decrease in current in nanopore by RPS technique also Coulter method of particle sizing and counting [14]. They related the change in measured current with the diameter of particle (d), nanopore diameter (D) and length of nanopore (L) mathematically expressed in equation a [14]:

$$\left|\frac{\delta I}{I}\right| = \frac{D}{L}\left[\frac{sin^{-1}\left(\frac{d}{D}\right)}{\sqrt{1-\frac{d}{D}}} - \frac{d}{D}\right] \quad (1)$$

Above equation can be approximated as, $\left|\frac{\delta I}{I}\right| = \frac{V_{particle}}{V_{pore}}$

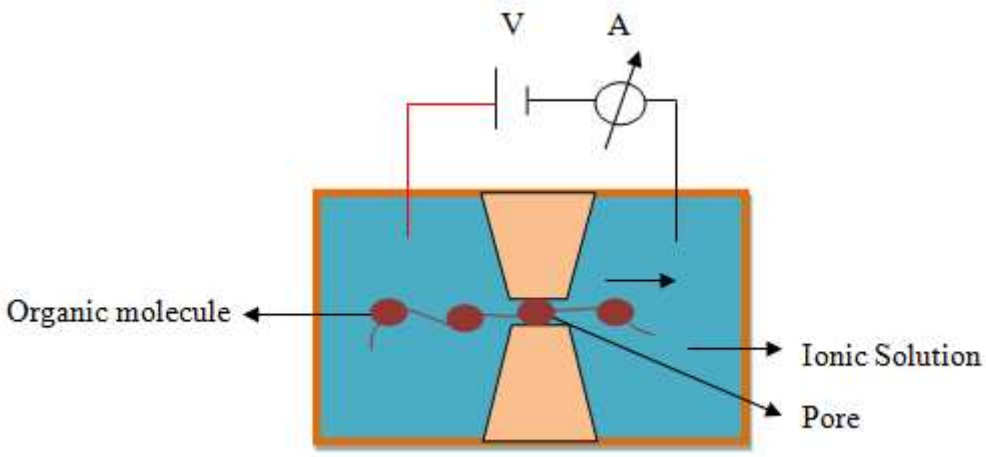

Figure 4: Typical connection for current by RPS in solid state nanopore. Biasing potential source (V) and an ammeter (A) are connected across the two chamber connected by a conducting ionic solution.

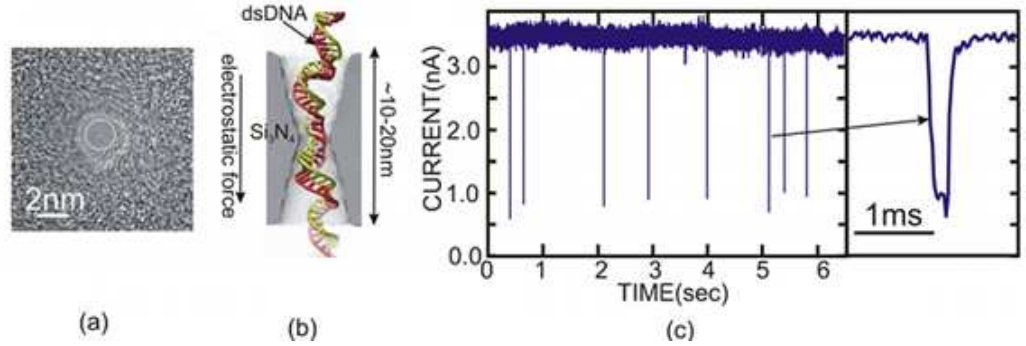

Figure 5: (a) A 2nm solid state nanopores in silicon nitride substrate. (b) Movement of double stranded DNA (dsDNA) within the nanopores. (c) Current measured during the dsDNA translocation within the nanopores, with 100mM KCl with 1.0V as applied bias potential across the nanopore. Current blockade is observed through the pore with change in current $\left|\frac{\delta I}{I}\right| > 0.78$ [15].

4. Low Frequency Noise Modeling

Low frequency $\frac{1}{f}$ noise also called as flickering noise, is the common fluctuating nose with power spectral density (PSD) proportional to $\frac{1}{f^{\gamma}}$, where γ is the current exponent which is close to 1, which takes the general form described by the normalized noise power (A) given by the equation:

$$A = S_I \frac{f}{I^2} \tag{2}$$

Where, S_I is the current power spectral density, f is the frequency and I is the average current.

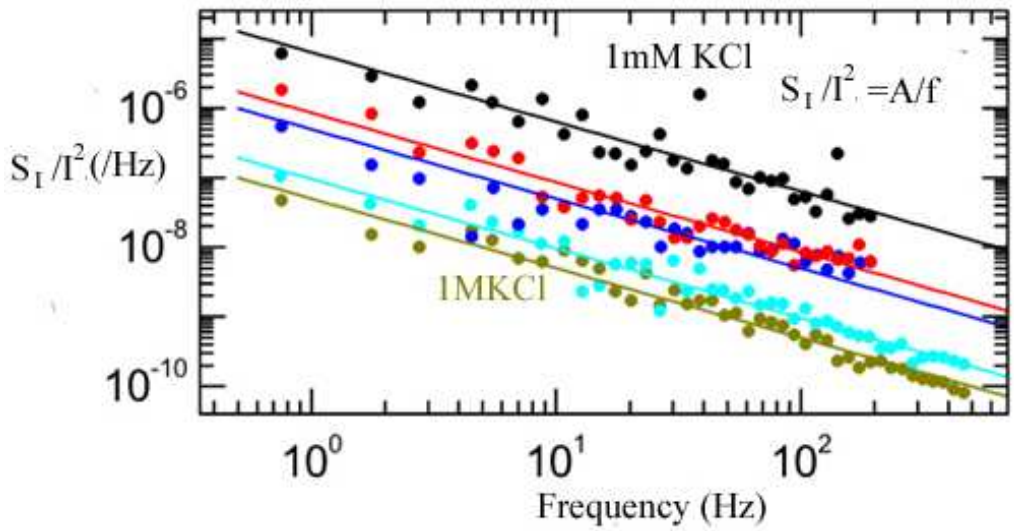

*Figure 6: Low frequency noise model for nanopore . Solid line fit is obtained for normalized noise power (A) range from 3.6 * 10^{-9} to 7*10^{-5} [16].*

As expected from eq. 2, the plot in fig. 6 clearly depicts the inverse relation of noise power spectral density with frequency. Also hold true for various ionic concentrations ranging from 1M KCl to 1mM KCl concentration. Noise power are found to be higher for low ion concentration within the nanopores, following the fact that noise power scales inversely with the number of carrier concentration within a nanopores (eq. 3). The solid line is the fit in accordance with Hooge's model, which will be discussed in following section.

Here, two different models of low frequency ($\frac{1}{f}$) flickering noise in solid state nanopores are described namely-surface trap model and Hooge's mobility fluctuation model.

(a) Hooge's Model (Mobility Fluctuation Model)

The Hooge's model for low frequency 1/f noise spectra is the linear relation between noise powers with the inverse number of charge carriers (N_c) [17] with α as the proportionality constant,

$$A_H = \frac{\alpha}{N_c} \tag{3}$$

In this model low frequency in solid state nanopores are described by the parameter α. It was first suggested to be constant with value of 2 * 10^{-3}, later found that depends on the quality of crystal. It fails to the situation when considering number of traps in the solid state nanopores surface under consideration

(b) Surface Charge Fluctuation Model (Based on Surface Traps)

This model considers surface of solid state nanopores made up oxide layer as the insulator, where surface charge fluctuation is inevitable due to surface traps which results in fluctuation in the measured ionic current. The amount of surface charge fluctuations due to surface charge traps (δq_t), and its power spectral density ($S_{q,t}$), as [17]

$$\delta q_t = \gamma * F(t) \tag{4}$$

$$S_{q,t} = \frac{\gamma^2}{f} \tag{5}$$

Where, γ is a proportionality constant reflecting the strength of fluctuations and F(t) is a dimensionless noise function with a $\frac{1}{f}$ power spectrum [17]. The normalized current noise power in terms of surface charge fluctuations is given as:

$$A = \left[\frac{\partial I}{\partial q}\right]^2 S_q \frac{f}{I^2} \tag{6}$$

Finally, assuming cylindrical geometry with length (L) and diameter (d) and G is the conductance of the nanopores [17],

$$A = \left[\frac{1}{\pi d L}\right]^2 \left[\frac{\partial I}{\partial \sigma}\right]^2 S_q \frac{f}{I^2} = \left[\frac{1}{\pi d L}\right]^2 \left[\frac{\partial G}{\partial \sigma}\right]^2 S_q \frac{f}{G^2} \tag{7}$$

For KCl as the ionic solution within the cylindrical nanopores, the ionic conductance (G) is given as:

$$G = \frac{\pi}{4}\frac{d^2}{L}\left[(\mu_K + \mu_{Cl}) n_{KCl} e + \mu_K \frac{4\sigma}{d}\right] \tag{8}$$

Where, $\mu_K \; and \; \mu_{CL}$ are the corresponding electrophoresis mobilities of potassium and chloride ions and n_{KCl} is the number density of potassium and chloride ions in the solution.

Differentiating G w.r.t σ yields:

$$\left(\frac{\partial G}{\partial \sigma}\right) = \frac{\pi d}{L}\mu_K \tag{9}$$

Finally, Normalized noise power for surface charge fluctuation originating from surface charge trap is found by replacing eq. 9 on eq. 7 as:

$$A_t = \left(\frac{\mu_K \gamma}{GL^2}\right)^2 \tag{10}$$

Comparison between Hooge's model and surface charge fluctuation model

Surface trap model doesn't fit into the normalized noise power curve for different KCl concentration rather fits for low concentration regime. But Hooge's model well fits in to the curve for both low and high concentration regime.

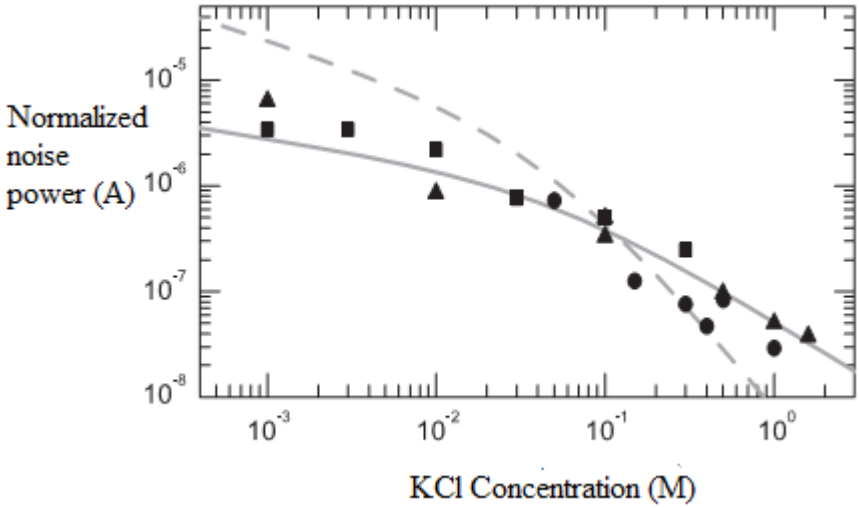

*Figure 7: Normalized noise power for nanopores with similar diameters for different KCl concentrations (1mM to 1.6M). Solid line is fitted with Hooge's law with fitted parameter (α) as 1.1 *10^{-4} eq. 3). Dashed line is fitted according to surface trap induced surface charge fluctuation model (fitted parameter is γ=3.1* 10^{-20} C eq. 10 where, L is 25nm) [17].*

Poor fitting for surface trap model can be elucidated by careful inspection of the eq. 3 and 10 describing the model- $A_t \propto \frac{1}{n_{KCl}^2}$, and Hooge's model (eq. 3)$A_H \propto \frac{1}{n_{KCl}}$. Hence, it's clear that at higher concentration of KCl we would see discrepancy of measured A_t by surface charge trapping model.

5. High Frequency Noise Model

Thermally excited charge carriers or carrier fluctuation in the conductor, is the origin of thermal noise or Johnson noise or Nyquist noise or white noise. For a single resistor, Johnson's noise is represented as the noiseless resistor (R) in parallel with the current noise source (I_{th}-Thevenized electrical circuit representation) in fig. 8 as illustrated below:

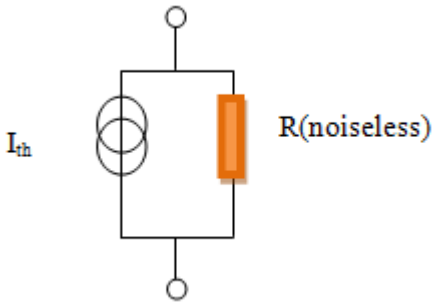

Figure 8: Typical Thevenized noise source (high frequency noise source) in parallel with noiseless resistor.

The corresponding current (S_I) and voltage spectral density (S_V) determined by Johnson noise is given as:

$$S_I = \left|\frac{1}{R}\right|^2 * S_V = |Y|^2 * S_V \tag{11}$$

$$S_V = 4k_BT\, Re(R) = 4k_BT\, Re\left(\frac{1}{Y}\right) \tag{12}$$

Where, k_BT represents the thermal energy.

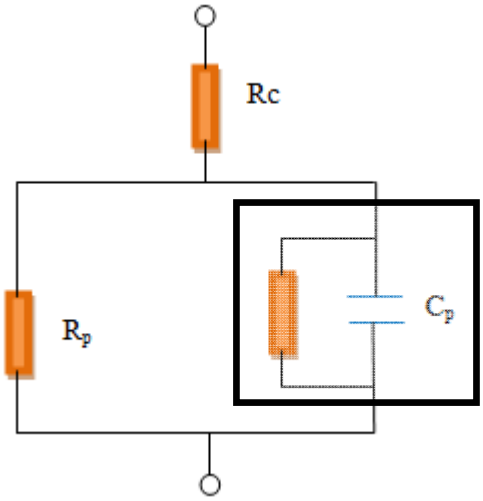

Figure 9: A typical equivalent electrical circuit representation of the nanopores sample.

A nanopores sample is equivalent with the Resistor (*Rp*). Resistor (*Rp*) is parallel with a capacitor (*Cp*) resulting from the liquid contact to the silicon chip containing the nanopores. The nonideal behavior of this capacitor by inclusion of admittance:

$$Y_s = w\, C_P\, D \tag{13}$$

Where, D is the dielectric loss constant. The circuit is in series with the resistor (*Rc*) that represents the resistance from the electrodes to the nanopores. To calculate the value of Ys, step voltage is applied to the nanopores sample and measure the current response [16].

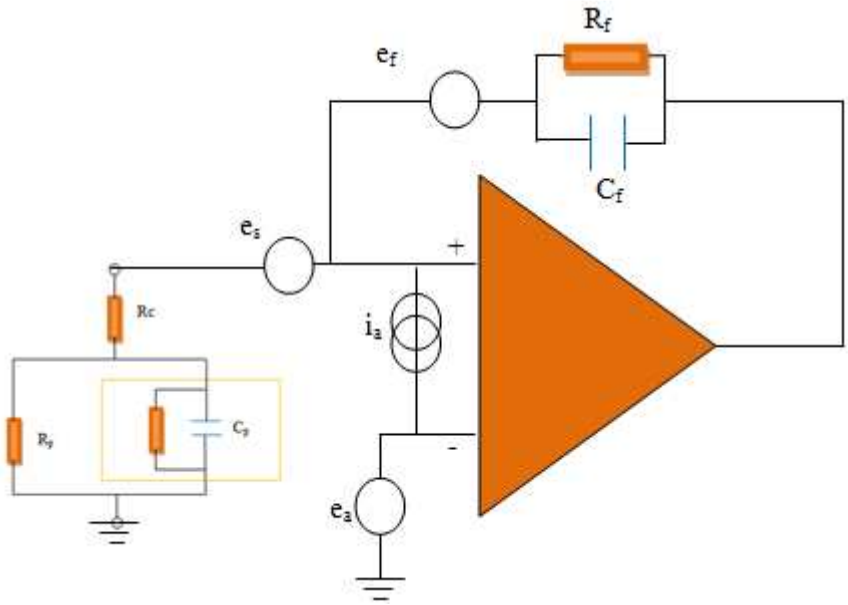

Figure 10: A nanopores is connected with the operational amplifier with feedback circuit.[16]

In above amplifier circuit, R_f and C_f are the feedback resistor and the capacitor, e_a and i_a are the voltage noise source and current noise source due to the operational amplifier (OA), e_f is the voltage noise source due to feedback circuit and e_s is the voltage noise source due to the nanopores sample. The OA generates noise with associated current and voltage power spectral densities of i_a and e_a respectively. The output current power spectral density following from eq. 13 is [16]:

$$S_I = i_a + |Ys|^2(e_a + e_s) + |Y_f|^2(e_a + e_f) \tag{14}$$

Where, Y_s and Y_f are the admittance of the nanopores sample and the feedback circuit.

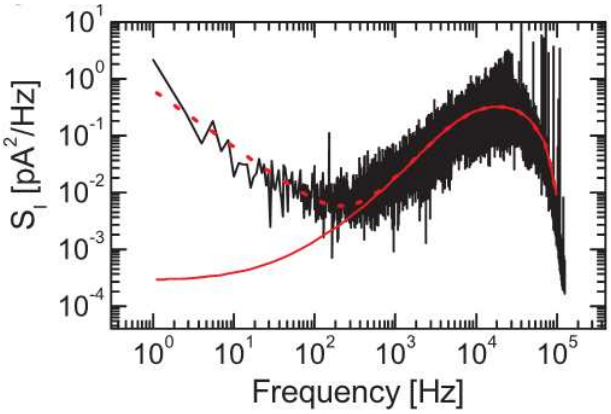

Figure 11: Black curve is the measured noise spectral density for 15.6nm diameter nanopores, red solid line is the calculated noise spectral density; red dashed line is result from addition of the measured low-frequency noise to calculated values. [16]

6. Signal to Noise Ratio for DNA Translocation

SNR is defines as: $SNR = \frac{|\Delta I|}{I_{noise,RMS}}$, where $I_{noise,RMS}$ is the root mean square current noise and $|\Delta I|$ is the absolute current change due to DNA translocation.

Mathematically,

$$I_{noise,RMS} = \left(\int_0^{BW} S_I df\right)^2 \quad (15)$$

Where, BW is the bandwidth of the signal and S_I is current spectral density. The DNA induced current change ΔI is found to be linearly proportional to the salt concentration, with DNA translocation resulting in either decrease (when [KCl]>0.4M or increase [KCl] < 0.4M) in ionic current, with bandwidth of 10 KHz.

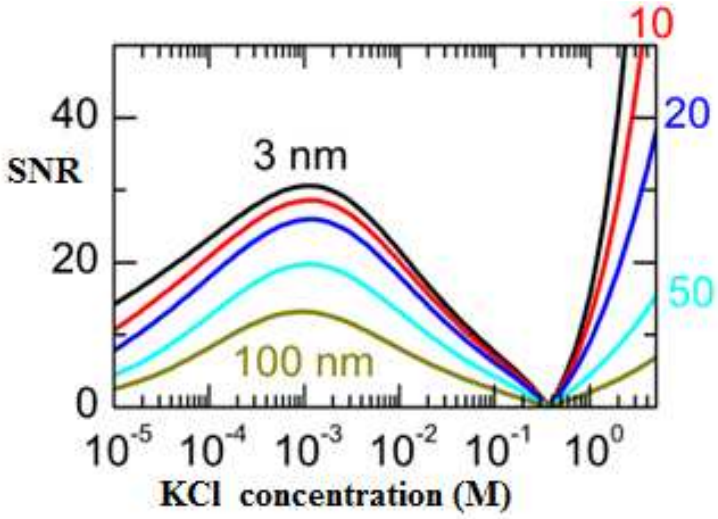

Figure 12: Signal to noise ratio (SNR) calculated for DNA translocation through 5 nanopores with diameter ranging from 3nm to 100 nm at different salt concentration [16].

Fig. 12 shows SNR as a function of KCl concentration for five different solid state nanopores. At very low salt concentration SNR decreases to almost zero because $|\Delta I|$ tends towards zero at 0.4M and increases reaching maximum at 10^{-3}M KCl. Further decrease in KCl concentration decreases the SNR because of lower voltage drom across nanopores. Lower voltage drop is due to the fact that series resistance (R_c) becomes equal to or larger than the pore resistance (R_p) [16]. We can clearly observe that, for smaller diameter nanopores, SNR is much better compared to larger nanopores. Is quite expected because amount of displace fluid in comparison to tube diameter is maximum for smaller diameter pores. Interesting observation is for large diameters SNR is higher at low concentration of KCl. Hence, for large nanopores (d > 20nm), measurement must be performed at low salt concentration.

7. Protein binding in DNA

Proteins constantly bind with proteins during transcription and replication during transfer of genomic information. Hence, nanopore could be an interesting tool for detection of protein modulated DNA. Fig. 13 is the schematic diagram for the detection of RecA protein coated DNA molecule while flowing between the nanopore in the KCl solution. RecA protein is a 38 Kilodalton protein *E. Coli* essential for the repair and maintenance of DNA.

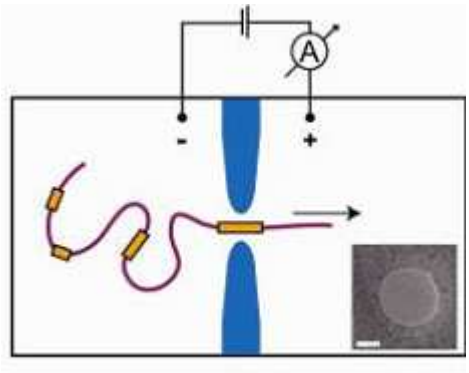

Figure 13: DNA molecule coated with RecA-Protein between ionic solutions, inset is the TEM image of 20nm nanopore [2].

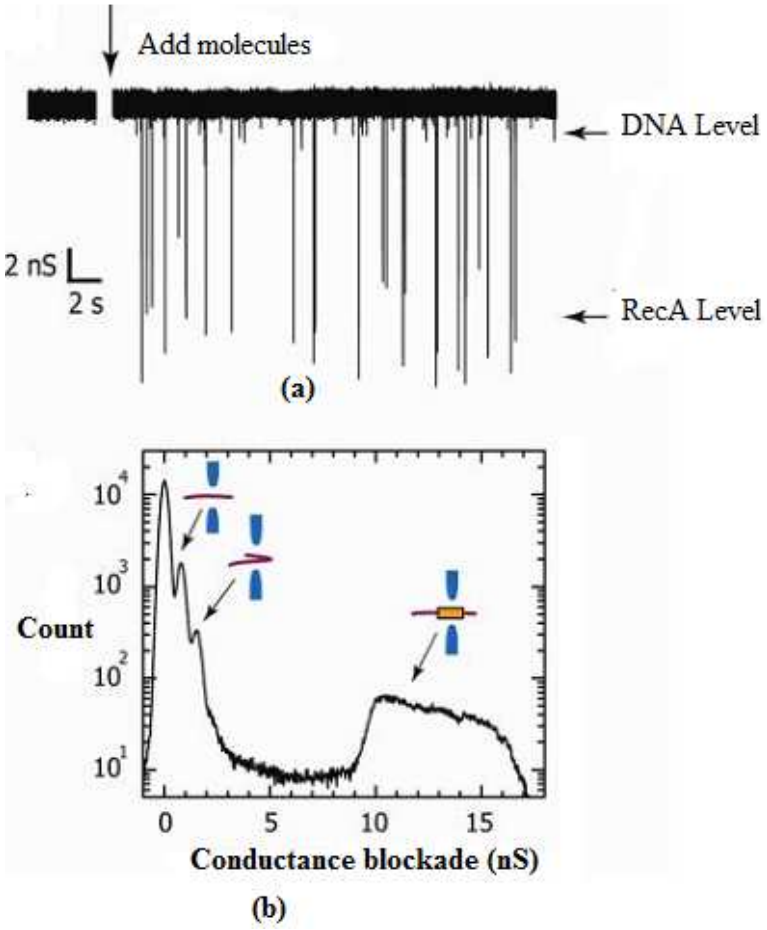

Figure 14: (a) Current measured across the nanopore during the transfer of RecA protein. (b)Conductance histogram for 2799 events at 60mV and each peak is for unfolded, folded and RecA coated DNA [2].

From fig. 14, conductance across the nanopores drops sharply for coated DNA molecule as compared with bare DNA. The further analysis of coated DNA depicts modulated current for different coating length (fig. 15).

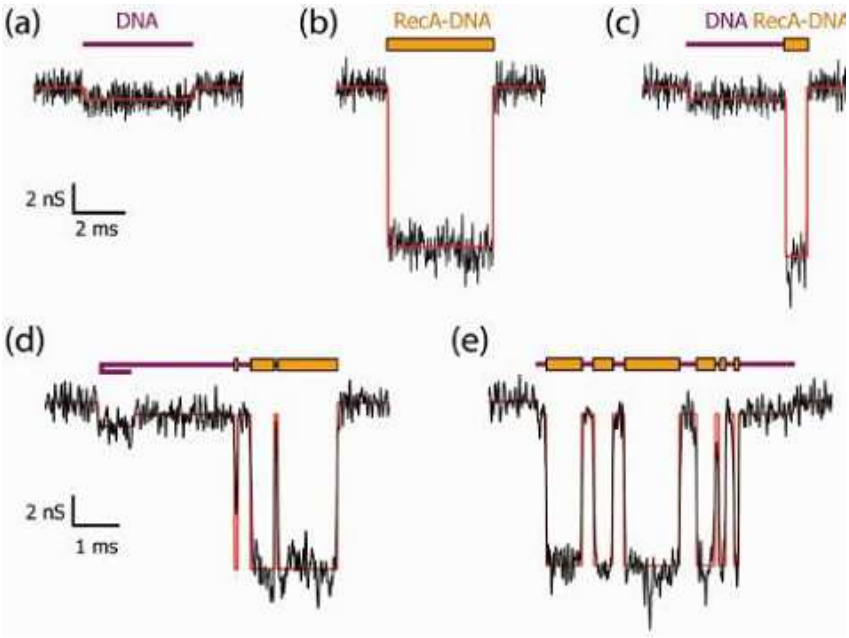

Figure 15: Conductance variation for DNA coated with proteins of different length, measured at 60mV [2].

The peaks at 0.8 to 1.6nS indicate the presence of one and two strands of dsDNA in the nanopore and the broad peak at 10-16nS represents the passage of RecA-coated DNA. The major issue is the resolution (smallest length of coated protein) of the measured conductance ($\Delta I/V$), because the difference between measured conductance due to coated and bare DNA is differing only in the orders of 10nS. The resolution along a DNA molecule of length(L) is defined as $\Delta l=L(\Delta t/\tau)$, where Δt is the minimum resolvable time set by the measurement bandwidth set by the measurement and τ is the total translocation time of the molecule. The resolution is directly dependent of the noise during measurement. Hence, it is necessary to reduce the noise below the threshold for accuracy of the measured current. Voltage dependent resolution of the structure exhibits structure as small as 8nm or 5 RecA monomers binding to 15 base pairs of DNA [2].

8. Reduction of noise in solid state nanopore

A gasket based nanopore has been proposed to decrease the noise in solid state nanopore [18]. In this approach, a nanopore silicon support chip is sandwiched by two silicone elastomers gaskets to for gigaohm range seal between two liquid reservoirs. A thin layer of PDMs is deposited on the S_iN_x nanopore. On other side electrodes are then to measure the current between the conductive liquid separated by a nanopore. The corresponding current and current spectral density is measured for different nanopores (either bare or covered with PDMS) and compared with the α-HL protein nanopore (fig. 17).

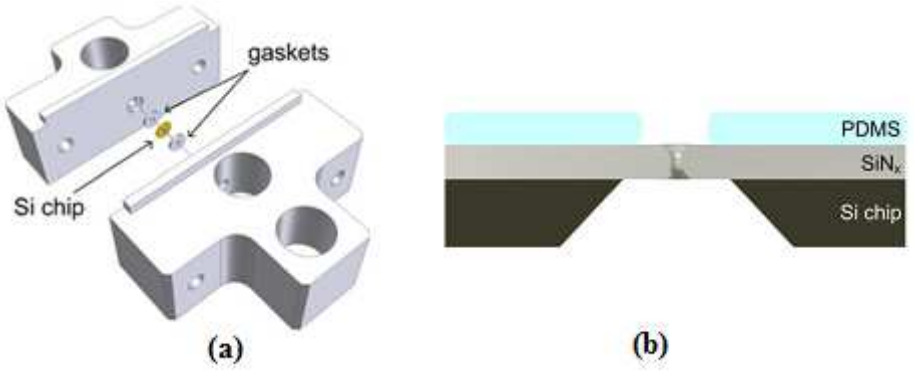

Figure 16: (a) Gasket based solid state nanopores. A silicon nanopore is supported with double gasket of elastomers, and (b) nanopores treated with a PDMS [18].

Noise power spectral density (S) can be broken down to respective components as expressed in the following equation [18]:

$$S = \alpha_1 + \alpha_2 f + \alpha_3 f^2 \, pA^2 Hz^{-1} \tag{16}$$

Where, f is the frequency in Hz. The constants parameters α_1(white noise component) arises from the constant thermal and shot noise of system, $\alpha_2$arises from dielectric noise associated with the capacitance of the Si/SiNx support chip and α_3 term arises from the pairing of thermal voltage noise with distributed capacitance of the system [18]. The measured noise power spectral density for different systems and the corresponding fitted curves are depicted in fig. 17. The fitted parameters are shown in table 1.

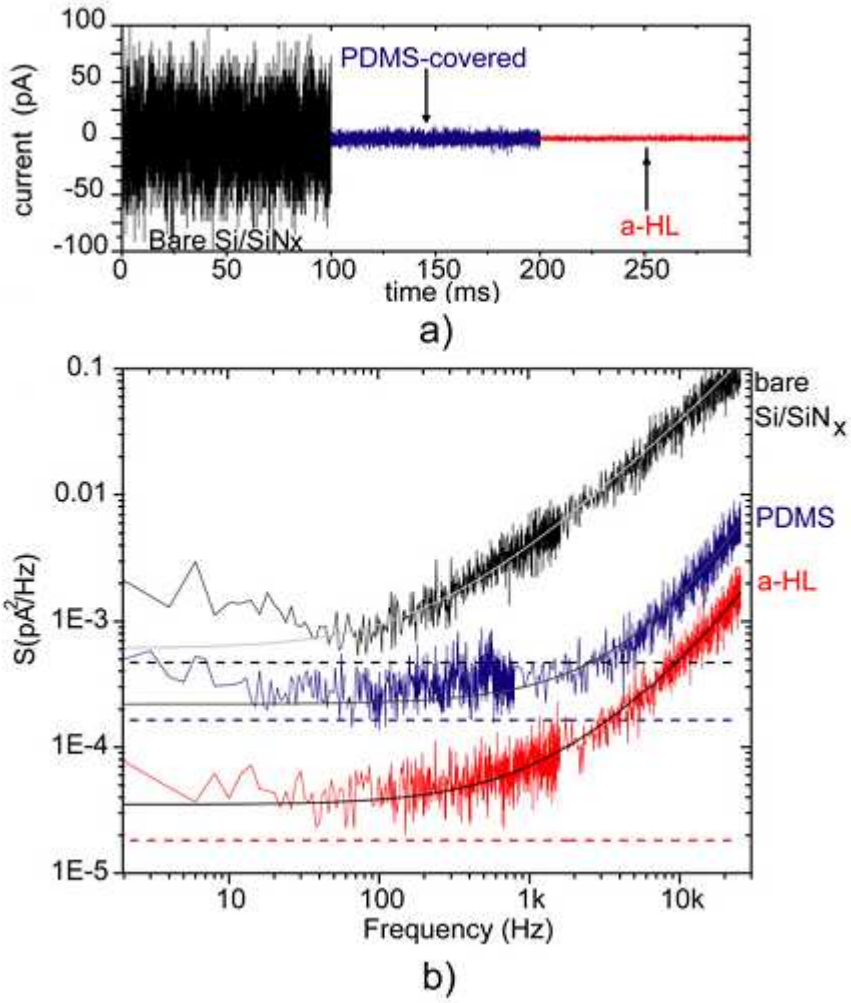

Figure 17: (a) Current measured for solid and noise power spectral density (b) for solid state SiNx bare (black) and covered with PDMS (blue), and the biological nanopores (red). The current measurement was performed (at 0 bias voltage of 1M KCl buffer solution) at 100Khz sampling rate using an Axopatch 200B amplifier with an SR785 signal analyser and the Bessel filter set at 100Khz [18].

Table 1: Corresponding fitting parameters obtained from fig. 17 (b) [18].

	a_1	a_2	a_3
Si	$6(\pm 10) \times 10^{-4}$	$3.4(\pm 0.3) \times 10^{-6}$	$5(\pm 1) \times 10^{-11}$
PDMS	$2.2(\pm 0.7) \times 10^{-4}$	$0.08(\pm 0.01) \times 10^{-6}$	$0.57(\pm 0.05) \times 10^{-11}$
α-HL	$0.39(\pm 0.04) \times 10^{-4}$	$0.035(\pm 0.002) \times 10^{-6}$	$0.12(\pm 0.01) \times 10^{-11}$

Fig. 17 clearly demonstrates the advantage of having PDMS layer on the nanopore. The major reason behind reduction of noise after having a PDMS is due to effect on α_2 parameter or reduction in dielectric noise, as observed in table 1. Since eq. 16 model doesn't consider any low frequency flickering noise ($1/f^{\alpha}$), the plots depicted in fig. 17 is well fitted only for high frequency.

Outlook

Is solid state nanopore really feasible and will enhance the current genomic technology? Is it possible to resolve the single DNA base pair? This review paper has answers to many critical issues towards the development of nanopores sensors-noise in solid state nanopores, SNR for DNA translocation through nanopores and detection of local protein along DNA molecule.

Development of scanning electron microscope had huge influence in nanopore technology by opening an avenue towards smaller and stable nanopores. However, the major issue is the presence of noise in solid state nanopores which directly influences the accuracy and sensitivity of measurement and measuring devices. E.g. signal to noise ratio of DNA translocation is influenced by noise from the nanopores, resulting in low resolution of measurement.

Initially, low frequency noise model considering - Hooge's model and Surface trap model, and later high frequency noise model is discussed in this paper. Hooge's model describes the low frequency noise in solid state nanopores with a parameter-α. Unfortunately, α is found to be varying with different nanopore material. Hence, a better model is necessary to describe the entire situation. The scientific community had always sought for improved model which would perfectly describe the nature of low frequency noise in solid state nanopores. In a concrete review of some application of solid state nanopore many interesting observations were made. E.g. DNA translocation analysis through nanopore depicted that smaller nanopore results in enhanced SNR compared with the larger one when experiment was carried with different salt concentrations. Additionally, for larger nanopores (d>20nm) measurement performed at low salt concentration yielded better SNR. In another application with bound protein along DNA, conductance of different RecA protein coated dsDNA was observed, depicting variation of conductance with different proteins length. Finally, in a novel approach with gasket based nanopore, PDMS treated SiN nanopore sensors exhibited enhanced performance compared with the bare nanopore. This phenomenon was due to the reduction of high frequency dielectric noise when nanopore was supported with PDMS.

Thus, solid state nanopore has huge potential towards single molecule DNA sequencing and reading the genome of the single cell and will certainly stand itself as the key technology in the field of genomics.

References

[1] Kasianowicz, J. J.; Brandin, E.;Branton, D.; Deamer, D. W.; Characterization of Individual Polynucleaotide Molecules Using a Membrane Channel, *Proc. Natl. Acad. Sci. U.S.A* 93, 13770-3 (1996).

[2] Dekker, C.; Kowalczyk, S. W.; Hall, A. R.; Detection of local protein structures along DNA using solid state nanopores, *Nano Lett. 10*, 324–8 (2010).

[3] Uram, J. D.; Ke, K.; Hunt, A. J; Mayer M.; Submicrometer Pore-Based characterization and Quantificaiton of Antibody-Virus Interactions. *Small* 2, 967-72 (2006).

[4] Saleh, O. A.; Sohn, L. L.; Quantitative Sensing of Nanoscale Colloids Using a Microchip Coulter Counter, *Rev. Sci. Instrum.* 72, 4449-51 (2001).

[5] Bezrukov, S. M.; Vodyanoy, I.; Parsegian, V. A.; Counting Polymers Moving through a Single Ion Channel, *Nature* 370, 279-81 (1994).

[6] Saleh, O. A.; Sohn, L. L.; Direct Detection of Antibody-Antigen Binding Using an on-Chip Artificial Pore, *Proc. Natl. Acad. Sci. U.S.A* 100, 820-4 (2003).

[7] Uram, J. D.; Ke, K.; Hunt, A. J; Mayer M.; Label-Free Affinity Assays by Rapid Detection of Immune Complexes in Submicrometer Pores, *Angew. Chem.. Int. Ed.* 45, 2281-5 (2006).

[8] Siwy, Z. S.; Ionic-Current Rectification in Nanopores and Nanotubes with Broken Symmetry, *Adv. Funct. Mater.* 16, 735-46 (2006).

[9] Butler, T. Z.; Pavlenok, M.; Ian, M. D., Niederweis, M. and Jens, H.; Gundlach, H.; Single-Molecule DNA Detection With an Engineered MspA Protein Nanopore, *Proc. Natl. Acad. Sci. U S A* 105(52), 20647–20652 (2008).

[10]Carbonaro. A; Sohn, L. L.; A Resistive Pulse Sensor Chip for Multianalyte Immunoassay, *Lab Chip* 5, 1155-60 (2005).

[11] Merchant, C. A.; Healy, K.; Wanunu, M.; Ray, V.; Peterman, N.; Bartel, J.; Fischbein, M. D.; Venta, K.; Luo, Z.; Johnson A. T. C.; Drndi, M.; DNA Translocation Through Graphene Nanopores, *Nano Lett. 10*, 2915–21 (2010).

[12] Li, J.; Stein, D.; McMullan, C.; Branton, D.; Aziz, M. J.; Golovchenko, J. A. Ion beam Sculpting at Nanometer Length Scales, *Nature* 412, 166-9 (2001)

[13] Dekker, C.; Krapf, D.; Wu, M.; Krapf, D.; My, W.; Smeets R. M; Zandbergen H. W.; Lemay, S. G.; Fabrication and characterization of Nanopore-based electrodes with Radii down to 2nm, *Nano Lett.* 6, 105-9 (2006).

[14] Deblois, R. W.; Bean, C. P.; Counting and sizing of submicron particles by the resistive pulse techniques, *Rev. Sci. Ins.* 41, 909-16 (1970).

[15] Dimitrov, V.; Mirasaidov, W.; Wang, D. Nanopores in solid-state membranes engineered for single molecule detection, *Nanotechnology* 21, 065502-23 (2010).

[16] Smeets, R. M. M.; Keyser, U. F.; Dekker, N. H.; Dekker,; C. Noise in solid state nanopores, *Proc. Natl. Acad. Sci. U S A* 105, 2, 417-21 (2008).

[17] Dekker, C.; Dekker, N.; Smeets, R. M.; Low Frequency noise in solid state nanopores, *Nanotechnology* 20, 095501-4 (2009).

[18] Cossa, V. T.; Trivedi, D.; Wigginn, M.; Jetha, N. N.; Marziali, A.; Noise analysis and reduction in solid-state nanopores, *Nanotechnology* 18, 305505-11 (2007).